

# FAST PYROLYSIS OF POPLAR WOOD SAWDUST WITH LA-CONTAINING SBA-15 CATALYST BY PY-GC/MS ANALYSIS

XIAOLI GU,<sup>\*,\*\*</sup> XU MA,<sup>\*</sup> LIXIAN LI,<sup>\*</sup> CHENG LIU,<sup>\*</sup> KANGHUA CHENG<sup>\*</sup> and  
ZHONGZHENG LI<sup>\*</sup>

<sup>\*</sup>College of Chemical Engineering, Nanjing Forestry University, Nanjing 210037, China

<sup>\*\*</sup>State Key Laboratory of Pulp and Paper Engineering, South China University of Technology, Guangzhou 510640, China

Received February 13, 2013

The catalyst was prepared by immobilizing lanthanum rare element on the periodic mesoporous channels of siliceous SBA-15. Powder X-ray diffraction data and ICP-AES revealed that the host retains its hexagonal mesoporous structure after immobilization and most of the lanthanum species are better dispersed in the calcinated materials. The surface area and pore size of La/SBA-15 were considerably decreased, indicating the intrapore confinement of the lanthanum species. La-containing SBA-15 catalyst was employed for catalytic cracking of Poplar Wood Sawdust (PWS) fast pyrolysis vapors, using analytical pyrolysis-gas chromatography/mass spectrometry (Py-GC/MS). The La/SBA-15 catalyst displayed prominent capabilities to crack the lignin-derived oligomers to phenol or monomeric phenolic compounds without the carbonyl group and unsaturated C-C bond on the side chain. Moreover, the catalyst also significantly decreased the linear aldehydes and decarbonylated furan compounds. In addition, the catalyst slightly decreased the acids, while benzene or aromatic derivative hydrocarbons were increased. The above catalytic capability of La/SBA-15 catalyst was enhanced with the introduction of La into SBA-15 catalyst.

**Keywords:** lanthanum containing SBA-15, poplar wood sawdust, Py-GC/MS

## INTRODUCTION

As a potential energy resource, poplar wood sawdust (PWS) waste contains various valuable substances derived from cellulose, hemicelluloses and lignin. Currently, the vast majority of PWS is burned without any industrial application. Only a small amount of PWS is decomposed with traditional elemental chlorine or chlorine dioxide, leading to the formation of poly-chlorinated compounds along with poly-phenolic residues. Consequently, increasing research efforts have been made over the past few years to develop a totally chlorine-free environmentally friendly process, for example, by the use of pyrolysis, which plays an important role in the thermochemical conversion of biomass materials to bioenergy.<sup>1-3</sup> The pyrolysis process is highly complex and depends on several factors, such as biomass composition and heating

rate.<sup>4</sup> Few detailed pyrolysis information that can predict product specification and yields on PWS pyrolysis was found in the available literature. The lack of data leads to difficulties in understanding emission behavior of PWS during the thermal treatment process.

Since the 1990s, the discovery of a new family of ordered mesoporous silica materials has sparked considerable interest because of their regular pore array with uniform pore diameter (2.0-8.0 nm), high surface area and pore volume.<sup>5</sup> In the family of mesoporous molecular sieves, SBA-15 exhibits larger pore sizes and thicker pore walls, compared with other materials.<sup>6</sup> Due to its mesoporous structure, higher wall thickness and good hydrothermal stability, SBA-15 is the most promising catalytic material, since it has been

successfully synthesized. On the other hand, with the development of instrumental analyzing methods, pyrolysis-gas chromatography/mass spectrometry (Py-GC/MS) is an important technique for biomass characterization, because it involves not only the compositional information of the complex component macromolecules, but also the characteristics of volatile pyrolysis products. Py-GC/MS has been successfully applied to evaluate the thermal decomposition behavior and pyrolysis products of polymers in detail, due to its rapidity, high sensitivity, and effective separation of complex mixture compounds.<sup>7-9</sup>

In the present work, we reported the synthesis of lanthanum-containing SBA-15 mesoporous molecular sieves by a direct synthesis method in an acid medium. The properties of La/SBA-15 were characterized by powder X-ray diffraction (XRD) and N<sub>2</sub> adsorption-desorption analysis. The objective of this study is to investigate the performance of SBA-15 and La/SBA-15 catalysts

for the catalytic cracking of PWS. The Py-GC/MS experiment was carried out as it allowed direct analysis of catalytic products. To the best of our knowledge, studies dealing with the use of immobilized La-containing SBA-15 for the pyrolysis of PWS have not been previously reported.

## EXPERIMENTAL

### Materials

The PWS sample was supplied by Nanjing Forestry University, department of Pulp and Paper Science. Prior to experiments, the sample was dried in an oven at 105 °C for 3 h, the original materials were crushed and pulverized to a size of <0.2 mm before they were analyzed. The results of the proximate analysis (moisture, ash, volatile content and fixed carbon of sawdust sample), ultimate analysis of the combustible fraction (in weight-by-weight percentage) and component analysis of the sample are shown in Table 1.

Table 1  
Proximate, ultimate and component analyses of the PWS sample

Proximate analysis <sup>a</sup> (wt%)		Ultimate analysis <sup>b</sup> (wt%)		Component analysis <sup>a</sup> (wt%)	
Moisture	9.6	Carbon	45.5	Cellulose	44.75
Ash	3.7	Hydrogen	6.26	Hemicellulose	16.73
Volatile matter	75.54	Nitrogen	1.04	Lignin	30.72
Fixed carbon <sup>c</sup>	11.15	Oxygen <sup>c</sup>	47.2	Extractive <sup>d</sup>	6.14

<sup>a</sup> on dry basis; <sup>b</sup> ash and moisture free; <sup>c</sup> estimated by difference; <sup>d</sup> determined according to the ASTM Standard Test Method E 1690-01

### Catalyst preparation

La/SBA-15 was prepared using a direct synthesis procedure, according to the procedure reported by Zhao *et al.*<sup>6</sup> with minor modifications. 2 g triblock poly(ethylene oxide)<sub>20</sub>-poly(propylene oxide)<sub>70</sub>-poly(ethylene oxide)<sub>20</sub> (P123, average molecular mass about 5800, Aldrich) and a certain amount of lanthanum nitrate (La(NO<sub>3</sub>)<sub>3</sub>·6H<sub>2</sub>O) were dissolved in a mixture of 35 mL of 2 mol·L<sup>-1</sup> HCl and 15 mL deionized water (pH≈1) under stirring, and then 4 g of tetraethyl orthosilicate (TEOS) was added to this solution (the molar ratio of La/Si = 5%). The mixture was kept under continuous agitation at 40 °C for 24 h. And the gel was transferred to a Teflon-lined stainless steel autoclave and aged at 100 °C for 24 h. The solid product was recovered by filtration and repeated washing with deionised water, followed by drying at 50 °C overnight. The P123 template was removed by calcinating at 550 °C for 8 h in air. The SBA-15 material without lanthanum species was also prepared as reported in Ref.<sup>5</sup> for comparison.

### Catalyst characterization

The La content of the catalysts was measured by inductively coupled plasma and an atomic emission spectroscopy (ICP-AES) system, which was performed on Optima 4300DV. Before any measurements were taken, the solid sample was dissolved in dilute HCl solution with a small amount of HF.

X-ray diffraction (XRD) diffractograms were performed on D5000 Siemens powder diffractometer equipped with copper anode. The scattering intensities were measured over an angle range of 0°<2θ<4°, with a step size Δ(2θ) = 0.02° and a step time of 8 s.

Nitrogen adsorption/desorption isotherms were measured on Micromeritics ASAP2010 at liquid N<sub>2</sub> temperature. Specific surface areas of the samples were calculated from the adsorption isotherms by the BET method and pore size distribution from the desorption isotherms by the Barrett-Joyner-Halenda (BJH) method.

### Py-GC/MS analysis

Pyrolysis-gas chromatography/mass spectrometry

(Py-GC/MS) system was employed to separate and identify the pyrolysis volatiles. For this purpose, a Frontier PY-2020-type pyrolyser was directly attached to a gas chromatography/mass spectrometer (6890GC/5973MSD, Agilent). In the characterization process, the pyrolysis temperature of 600 °C was used. The chromatographic separation of the volatile products was performed using an Agilent HP-5 capillary column (30 m×0.25 mm×0.25 µm film thickness). Before the chromatographic separation, the temperature of the chromatographic column was progressively increased as follows: (i) 50 °C for 5 min; (ii) from 50 to 280 °C at a rate of 5 °C/min; (iii) the capillary column was maintained at 280 °C for about 15 min. Helium was used as carrier gas at a constant flow of 1.0 mL/min. The GC inlet was 300 °C and a split ratio of 20:1 was used. Mass spectra were recorded under electron ionization (70 eV) with the *m/z* range: 40-550 au. Peak identification was carried out with the NIST mass spectral library and literature.

## RESULTS AND DISCUSSION

### Catalyst properties

XRD patterns of calcinated SBA-15 and La/SBA-15 are shown in Figure 1. It exhibits three well resolved diffraction peaks with *d* = 10.3, 6.2 and 5.3 nm, which can be indexed as the (100), (110) and (200) reflections associated with *p* 6 mm hexagonal symmetry;<sup>10</sup> *d* (100) spacing of 10.3 nm corresponds to a large unit cell parameter *a* = 11.9 nm ( $a_0 = 2 \times d_{100} / \sqrt{3}$ ). Figure 1b shows the XRD La-containing SBA-15 and the reflections are marginally shifted toward 2θ values, which confirmed the immobilization of the La complex within the ordered SBA-15 structure.<sup>11</sup>

In the N<sub>2</sub> adsorption-desorption isotherms for siliceous SBA-15 and La/SBA-15 (Figure 2), typical irreversible type IV adsorption isotherms with a H1 hysteresis loop, as defined by IUPAC,<sup>12</sup> were observed. This H1-type hysteresis loop suggests that the material has regular mesoporous channels with narrow Gaussian pore size

distribution centered at 7.2 nm for siliceous SBA-15, at 6.3 nm for La/SBA-15 (Figure 3). In fact, the main pore diameter decreased as the percentage of lanthanum species increased, which is in agreement with the results published by other authors.<sup>13,14</sup>

The composition of solid products determined by ICP-AES is listed in Table 2. The results also show that the content of La in the solid sample measured by ICP-AES is obviously lower than that of the gel mixture, indicating a very small quantity of the solubility of lanthanum nitrate in the strong acidic medium. This indicates that the lanthanum species in the gel cannot be introduced completely into SBA-15 under some acidic conditions.

### Catalytic experiments

To get some insights on the formation of volatile organic decomposition products, thermal degradation process was performed by Py-GC/MS and Figure 4 shows the detailed volatile products from the pyrolysis of PWS with different catalysts. GC/MS is only able to analyze the volatile compounds in the pyrolysis vapors, which are mixtures of volatile compounds and non-volatile oligomers (known as pyrolytic lignins, mainly tri- and tetramers<sup>15</sup>). More than 100 peaks were displayed on the chromatograms, and the main compounds identified were listed in Table 3, with names, retention times, molecular formulas, molecular weights, and group types of sixty-four compounds present in the largest amounts detected by Py-GC/MS.

As the pyrolysis products were a mixture of a number of organic volatile species, these species were roughly grouped into the following categories: carbonyls (including aldehyde, ketone, acid and ester), furans, hydroxyls (mainly phenolic derivatives), benzene or aromatic derivatives and others.

Table 2  
Physicochemical properties of SBA-15 and La/SBA-15 materials

Sample	(La/Si) <sup>a</sup> gel(%)	(La/Si) <sup>b</sup> cal(%)	Total S <sub>BET</sub> <sup>c</sup> (m <sup>2</sup> /g)	Total D <sub>v</sub> <sup>d</sup> (m <sup>3</sup> /g)	D <sub>p</sub> <sup>e</sup> (nm)	a <sub>0</sub> <sup>f</sup> (nm)
SBA-15	-	-	780	1.1	7.2	10.6
La/SBA-15	5	1.18	566	0.9	6.3	11.9

<sup>a</sup> La/Si (molar ratio) in gel mixture; <sup>b</sup> La/Si (molar ratio) after calcinations, obtained by ICP analysis; <sup>c</sup> BET specific surface area; <sup>d</sup> Total pore volumes were obtained at *P/P*<sub>0</sub> = 0.99; <sup>e</sup> BJH pore diameter calculated from the desorption branch; <sup>f</sup> a<sub>0</sub> calculated by *d*<sub>100</sub>,  $a_0 = 2 \times d_{100} / \sqrt{3}$

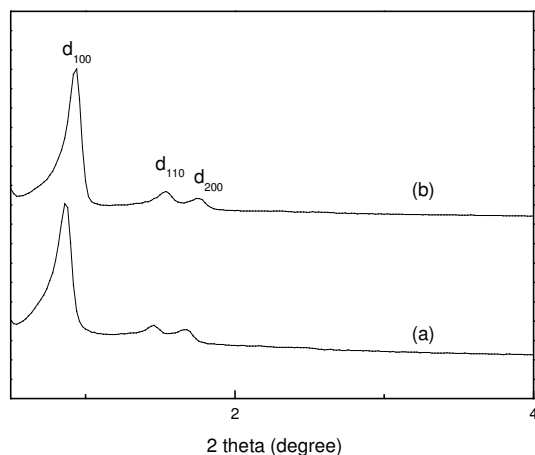


Figure 1: Powder XRD patterns of calcined SBA-15 (a) and La/SBA-15 (b)

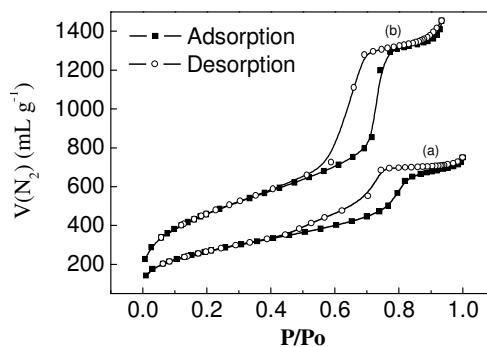


Figure 2: Nitrogen adsorption-desorption isotherms for SBA-15 (a) and La/SBA-15 (b)

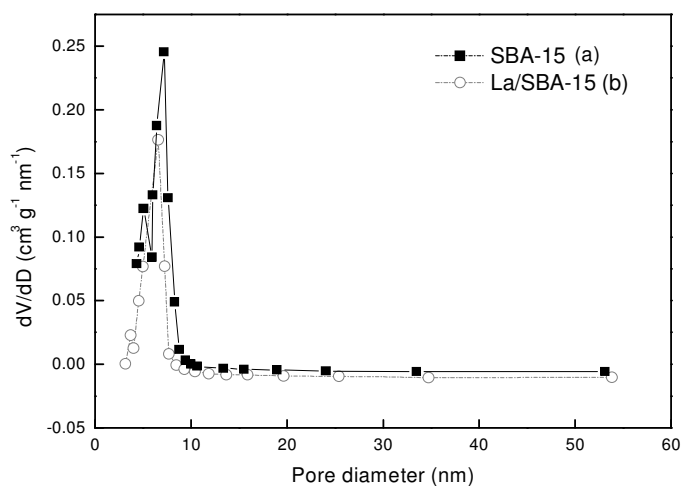


Figure 3: Pore size distribution patterns for SBA-15 (a) and La/SBA-15 (b)

Table 3  
Pyrolysis products of PWS by Py-GC/MS

No.	R.T. (min)	Name of compound	Formulae	MW (g/mol)	Type
1	1.82	methanol	CH <sub>4</sub> O	32	alcohol
2	2.20	acetaldehyde	C <sub>2</sub> H <sub>4</sub> O	44	aldehyde
3	2.35	furan	C <sub>4</sub> H <sub>4</sub> O	68	furan
4	2.73	methyl acetate	C <sub>3</sub> H <sub>6</sub> O <sub>2</sub>	74	ester
5	3.65	acetone	C <sub>3</sub> H <sub>6</sub> O	58	ketone
6	3.80	benzene	C <sub>6</sub> H <sub>6</sub>	78	benzene
7	4.03	hydroxyacetaldehyde	C <sub>2</sub> H <sub>4</sub> O <sub>2</sub>	60	aldehyde
8	4.10	2-methyl furan	C <sub>5</sub> H <sub>6</sub> O	82	furan
9	4.94	2,3-butanedione	C <sub>4</sub> H <sub>6</sub> O <sub>2</sub>	86	ketone
10	5.77	acetic acid	C <sub>2</sub> H <sub>4</sub> O <sub>2</sub>	60	acid
11	6.08	3-buten-2-one	C <sub>5</sub> H <sub>8</sub> O	84	ketone
12	6.61	propanoic acid	C <sub>3</sub> H <sub>6</sub> O <sub>2</sub>	74	acid
13	7.37	1-hydroxy-2-propanone	C <sub>3</sub> H <sub>6</sub> O <sub>2</sub>	74	ketone
14	7.59	toluene	C <sub>7</sub> H <sub>8</sub>	92	benzene

15	8.05	2-butenal	C <sub>4</sub> H <sub>6</sub> O	70	aldehyde
16	9.19	1-hydroxy-2-butanone	C <sub>4</sub> H <sub>8</sub> O <sub>2</sub>	88	ketone
17	9.49	acetoxyacetic acid	C <sub>4</sub> H <sub>6</sub> O <sub>4</sub>	118	acid
18	10.25	methyl pyruvate	C <sub>4</sub> H <sub>6</sub> O <sub>3</sub>	102	other
19	10.71	2,3,5-trimethylfuran	C <sub>7</sub> H <sub>10</sub> O	110	furan
20	12.30	styrene	C <sub>8</sub> H <sub>8</sub>	104	benzene
21	12.68	furfural	C <sub>5</sub> H <sub>4</sub> O <sub>2</sub>	96	furan
22	12.99	2-furanmethanol	C <sub>5</sub> H <sub>6</sub> O <sub>2</sub>	98	furan
23	13.59	ethylbenzene	C <sub>8</sub> H <sub>10</sub>	106	benzene
24	14.20	2-propylfuran	C <sub>7</sub> H <sub>10</sub> O	110	furan
25	16.25	1,2-cyclopentanedione	C <sub>5</sub> H <sub>6</sub> O <sub>2</sub>	98	ketone
26	17.32	3-methyl-2,5-furandione	C <sub>5</sub> H <sub>6</sub> O <sub>2</sub>	98	furan
27	17.77	1-ethyl-3-methyl-benzene	C <sub>9</sub> H <sub>12</sub>	120	benzene
28	18.53	5-methyl-furaldehyde	C <sub>6</sub> H <sub>6</sub> O <sub>2</sub>	110	furan
29	18.76	phenol	C <sub>6</sub> H <sub>6</sub> O	94	phenol
30	19.82	2-methyl-phenol	C <sub>7</sub> H <sub>8</sub> O	108	phenol
31	20.51	2H-pyran-2,6-(3H)-dione	C <sub>5</sub> H <sub>4</sub> O <sub>3</sub>	112	other
32	21.27	4-methyl-phenol	C <sub>7</sub> H <sub>8</sub> O	108	phenol
33	21.64	2-methoxy-phenol	C <sub>7</sub> H <sub>8</sub> O <sub>2</sub>	124	phenol
34	22.02	4-ethyl-phenol	C <sub>8</sub> H <sub>10</sub> O	122	phenol
35	23.39	2-methoxy-4-methyl-phenol	C <sub>8</sub> H <sub>10</sub> O <sub>2</sub>	138	phenol
36	24.83	1,2-benzenediol	C <sub>6</sub> H <sub>6</sub> O <sub>2</sub>	110	ketone
37	26.05	4-propyl-phenol	C <sub>9</sub> H <sub>12</sub> O	136	phenol
38	26.20	2,3-dihydroxy-2-methyl-4-pyrone	C <sub>6</sub> H <sub>6</sub> O <sub>4</sub>	142	other
39	26.28	5-(hydroxymethyl)-2-furaldehyde	C <sub>6</sub> H <sub>6</sub> O <sub>3</sub>	126	furan
40	26.43	7-methoxybenzofuran	C <sub>9</sub> H <sub>8</sub> O <sub>2</sub>	148	furan
41	26.73	2-methoxy-4-ethyl-phenol	C <sub>9</sub> H <sub>12</sub> O <sub>2</sub>	152	phenol
42	27.19	2-methoxy-4-vinyl-phenol	C <sub>9</sub> H <sub>10</sub> O <sub>2</sub>	150	phenol
43	29.70	2-methoxy-4-propyl-phenol	C <sub>10</sub> H <sub>14</sub> O <sub>2</sub>	166	phenol
44	29.85	2-methoxy-4-(2-propyl)-phenol	C <sub>10</sub> H <sub>14</sub> O <sub>2</sub>	166	phenol
45	30.38	2,6-dimethoxy-phenol	C <sub>8</sub> H <sub>10</sub> O <sub>3</sub>	154	phenol
46	30.99	4-methyl-1,2-benzenediol	C <sub>7</sub> H <sub>8</sub> O <sub>2</sub>	124	ketone
47	31.29	1-methyl-naphthalene	C <sub>11</sub> H <sub>10</sub>	142	benzene
48	31.82	2-methoxy-4-propenyl-phenol	C <sub>10</sub> H <sub>12</sub> O <sub>2</sub>	164	phenol
49	33.87	(E)-2-methoxy-4-propenyl-phenol	C <sub>10</sub> H <sub>12</sub> O <sub>2</sub>	164	phenol
50	34.86	4-hydroxy-3-methoxy-benzaldehyde	C <sub>8</sub> H <sub>8</sub> O <sub>3</sub>	152	aldehyde
51	35.32	1,2,4-trimethoxy-benzene	C <sub>9</sub> H <sub>12</sub> O <sub>3</sub>	168	benzene
52	36.68	5-tert-butyl-1,2,3-benzenetriol	C <sub>10</sub> H <sub>14</sub> O <sub>3</sub>	182	phenol
53	37.14	1-(3-hydroxy-4-methoxyphenyl)-ethanone	C <sub>9</sub> H <sub>10</sub> O <sub>3</sub>	166	ketone
54	38.13	levoglucosan	C <sub>6</sub> H <sub>10</sub> O <sub>5</sub>	162	other
55	38.96	3,5-dimethoxyacetophenone	C <sub>10</sub> H <sub>12</sub> O <sub>3</sub>	180	ketone
56	39.19	6-methoxy-3-methylbenzofuran	C <sub>10</sub> H <sub>10</sub> O <sub>2</sub>	162	furan
57	41.69	4-allyl-2,6-dimethoxy-phenol	C <sub>11</sub> H <sub>14</sub> O <sub>3</sub>	194	phenol
58	42.15	4-hydroxy-3,5-dimethoxy-benzaldehyde	C <sub>9</sub> H <sub>10</sub> O <sub>4</sub>	182	aldehyde
59	42.76	1-(4-hydroxy-3,5-dimethoxyphenyl)-ethanone	C <sub>10</sub> H <sub>12</sub> O <sub>4</sub>	196	ketone
60	44.05	1-(4-hydroxy-3,5-dimethoxyphenyl)-2-propanone	C <sub>10</sub> H <sub>12</sub> O <sub>3</sub>	180	ketone
61	44.58	4-((1E)-3-hydroxy-1-propenyl)-2-methoxyphenol	C <sub>10</sub> H <sub>12</sub> O <sub>3</sub>	180	phenol
62	45.19	4-hydroxy-2-methoxycinnamaldehyde	C <sub>10</sub> H <sub>10</sub> O <sub>3</sub>	178	aldehyde
63	45.49	1-(2,6-dihydroxy-4-methylphenyl)-1-butanone	C <sub>11</sub> H <sub>15</sub> O <sub>3</sub>	195	ketone
64	45.87	3,5-dimethoxy-4-hydroxycinnamaldehyde	C <sub>11</sub> H <sub>12</sub> O <sub>4</sub>	208	aldehyde

As shown in Figure 5, the yield of phenolic and aromatic derivatives increased, while the yield of carbonyls, mainly aldehydes, and furans decreased with SBA-15 and La/SBA-15 catalysts. Especially, the highest yield of phenolics compounds was

obtained for La/SBA-15, due to its highest amount of acid sites.<sup>16,17</sup> Acid sites can crack the PWS particles with large molecules more easily, resulting in higher phenolics yields. Therefore, the use of La/SBA-15 having a greater number of acid sites

resulted in a larger phenolic compounds yield.

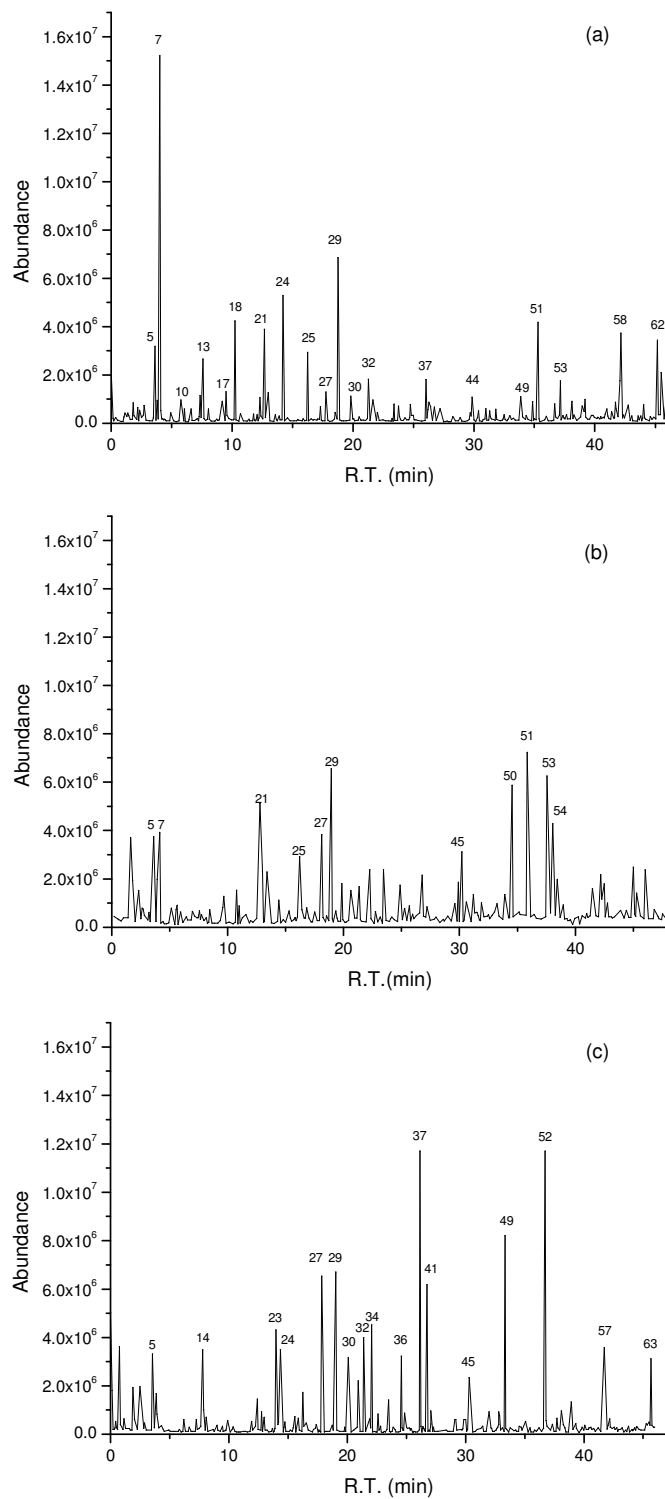


Figure 4: Py-GC/MS detection of gaseous products evolved from pyrolysis of PWS (a) no catalyst, (b) SBA-15 catalyst, (c) La/SBA-15 catalyst

The catalytic effects on major hydroxylic products, except trace amount methanol, are shown in Figure 6, and were classified into C<sub>6</sub>-C<sub>11</sub> six groups. It was shown that the yield of phenolics was the highest with the use of La/SBA-15 catalyst and the yields of light phenolics, such as C<sub>6</sub>-C<sub>8</sub> phenolics, increased slightly, while heavy phenolics including C<sub>9</sub>-C<sub>10</sub> phenolics increased greatly. All phenolic compounds were increased after catalysis, e.g., for C<sub>10</sub> phenolics, La/SBA-15 catalytic activity was 5.60 times greater than that for noncatalysis and 4.14 times greater than that of SBA-15 catalyst. Notably, some of the products, which were not detected in noncatalytic pyrolytic products, were formed after catalysis, such as 4-ethyl-phenol, 2-methoxy-4-ethyl-phenol and 2,6-dimethoxy-phenol, while the yield of 4-propyl-phenol, 2-methoxy-4-propenyl-phenol and 5-tert-butyl-1,2,3-benzenetriol increased greatly with La/SBA-15 catalysis. With regard to the pyrolysis vapors catalyzed by SBA-15, the yields of phenolics did not show very significant changes. This implied that La-containing SBA-15 catalyst could promote the cracking of PWS into phenolic compounds, which was in concordance with the literature report.<sup>18</sup> In this study, phenolics are considered to be valuable products because they can be used for production of the phenolic resins and other petrochemical products. Therefore, La/SBA-15 can be a good catalyst for production of phenolic compounds *via* pyrolysis of PWS.

Besides the phenolic products, the catalytic effects of other major products are also shown in Figures 7-9.

The effects of catalysts on benzene or aromatic

derivatives yield are presented in Figure 7. By applying catalysts, the yields of aromatics, especially C<sub>8</sub>-C<sub>9</sub> aromatic derivatives, increased, because it has been reported that acidity increased the production of aromatics,<sup>16,19</sup> the increase of aromatic yields for La/SBA-15 can be ascribed to its high acidity. Noncatalytic fast pyrolysis of the PWS generated a small amount of benzene or aromatic derivatives. After catalysis, more hydrocarbons were formed, such as styrene and ethylbenzene in C<sub>8</sub> group with La/SBA-15 catalysis. Even for SBA-15 catalyst, 1-ethyl-3-methyl-benzene and 1,2,4-trimethoxy -benzene increased greatly, compared with noncatalytic results.

Furans were detected in the pyrolytic products, as illustrated in Figure 8. Previous studies have also demonstrated that furans are dehydrated products of carbohydrates,<sup>20-22</sup> while the compounds that contained carbonyl groups, especially the aldehyde group, were decreased dramatically. For example, the furfural was decreased from 24.91% in the noncatalytic pyrolytic products to 10.04% in the La/SBA-15-catalyzed products. Some other compounds, such as 5-(hydroxymethyl)-2-furaldehyde and 7-methoxybenzofuran, were completely eliminated. Meanwhile, the lightest furan was increased considerably, that is, the peak area % of furan reached as high as 21.06% after catalysis by La/SBA-15. The result suggested that La/SBA-15 catalyst would enhance the value of bio-oil by cracking the furan compounds through decarbonylation to produce light ones, which have significant chemical application values.

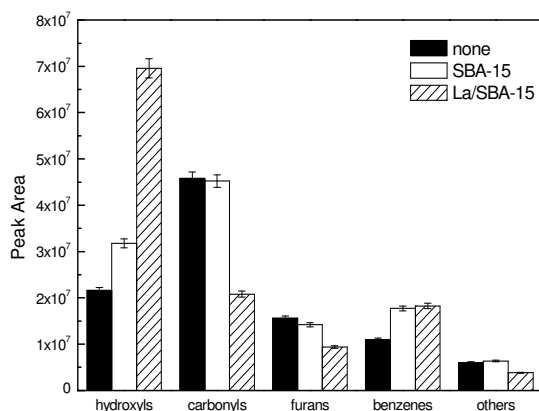


Figure 5: Distribution of pyrolysis products from Py-GC/MS ion chromatograms

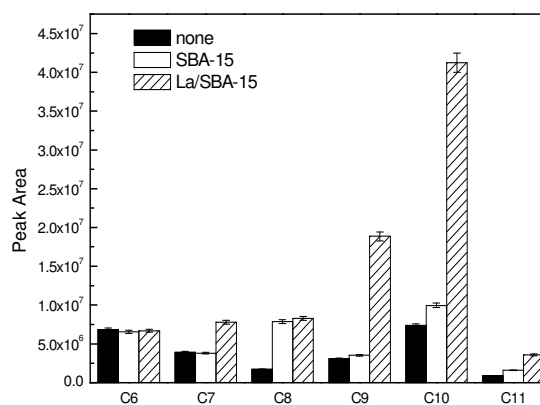


Figure 6: Catalytic effects on phenolic compounds

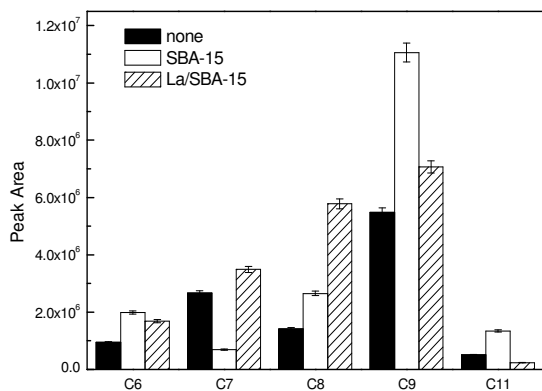


Figure 7: Catalytic effects on aromatic compounds

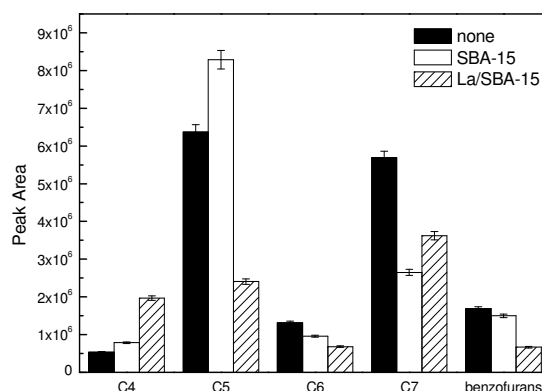


Figure 8: Catalytic effects on furan compounds

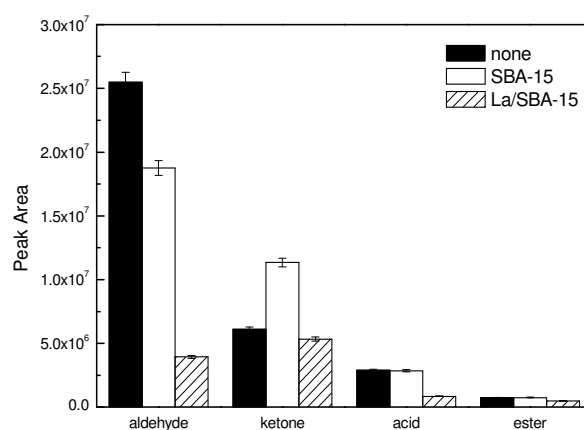


Figure 9: Catalytic effects on carbonylic compounds

Attention should be given to the carbonyls, because carbonyls, especially aldehydes, are mainly responsible for producing tar. In addition to the linear aldehydes, some furan and phenolic products also contained the aldehyde group. It is clearly indicated in the above results that the total aldehydes were decreased to a very small content after catalysis, which is obviously beneficial for improving the stability of the catalytic bio-oils. On the other hand, La/SBA-15 catalysts decreased the yields of acids. Undoubtedly, acids are undesirable products in bio-oil because of their corrosiveness, high yields of acids make bio-oil difficult to be used as a fuel. Therefore, the results indicated that the La/SBA-15 catalyst showed prominent catalytic activity, compared to literature reports.<sup>7,23,24</sup>

On the basis of the above results, it may be noted that the La/SBA-15 catalyst showed a prominent activity for production of phenolics, which was also effective to remove the carbonyl group from the benzene ring compounds, indicative

of its decarbonylation activity. In addition, fast pyrolysis of PWS also generated cyclopentanones, esters, and pyrans, which were all present in low content even after catalysis. Many reactions might contribute to the catalytic effects, and the reduction of the unsaturated C-C bond suggested that La/SBA-15 might have some hydrotreating capability. Further studies are required to reveal the mechanism involved in this process.

## CONCLUSION

For the first time we have demonstrated that mesoporous La/SBA-15 acts as an efficient catalyst for fast pyrolysis of poplar wood sawdust. The active La species seemed to be stabilized within the mesoporous host, rendering unusual catalytic activity. The result is attributed to the presence of isolated hydroxyl groups and the meso-micro pore architecture, which provides an ideal environment for the reaction.

After catalysis, the pyrolytic lignins in PWS

were cracked to monomeric phenols, which were further converted to phenols without the carbonyl group and the unsaturated C-C bond on the side chain and the furans were decarbonylated to form light furan compounds. Moreover, linear aldehydes were significantly decreased, while the acids were slightly decreased. Benzene or aromatic derivatives were all increased. The catalytic activity of La/SBA-15 was better than that of SBA-15 catalyst. The La/SBA-15 catalysts also increased the monomeric phenolic compounds remarkably, while phenolics are useful platform chemicals.

**ACKNOWLEDGEMENTS:** A Project Funded by the Priority Academic Program Development of Jiangsu Higher Education Institutions and supported by Jiangsu Key Lab of Biomass-based Green Fuels and Chemicals. The authors are grateful to Natural Science Fund in Jiangsu Province of China (BK20130963), the opening funding of State Key Laboratory of Pulp and Paper Engineering in South China University of Technology (201209), Forestry Industry Research Special Funds for Public Welfare project (201104032).

## REFERENCES

- <sup>1</sup> R. Bilbao, J. F. Mastral, M. E. Aldea, J. Ceamanos, *J. Anal. Appl. Pyrol.*, **39**, 1 (1997).
- <sup>2</sup> J. L. Banyasz, S. Li, J. L. Lyons-Hart, K. H. Shafer, *J. Anal. Appl. Pyrol.*, **57**, 2 (2001).
- <sup>3</sup> M. Asmadi, H. Kawamoto, S. Saka, *J. Anal. Appl. Pyrol.*, **92**, 2 (2011).
- <sup>4</sup> R. T. Rao, A. Sharma, *Energy*, **23**, 11 (1998).
- <sup>5</sup> C. T. Kresge, M. E. Leonowicz, W. J. Roth, J. C. Vartuli, J. S. Beck, *Nature*, **359**, 6397 (1992).
- <sup>6</sup> D. Y. Zhao, J. L. Feng, Q. S. Huo, N. Melosh, G. H. Fredrickson *et al.*, *Science*, **279**, 5350 (1998).
- <sup>7</sup> Q. Lu, W. Z. Li, D. Zhang, X. F. Zhu, *J. Anal. Appl. Pyrol.*, **84**, 2 (2009).
- <sup>8</sup> Q. Lu, X. C. Yang, C. Q. Dong, Z. F. Zhang, X. M. Zhang *et al.*, *J. Anal. Appl. Pyrol.*, **92**, 2 (2011).
- <sup>9</sup> M. Zhang, F. L. P. Resende, A. Moutsoglou, D. E. Raynie, *J. Anal. Appl. Pyrol.*, **98**, 1 (2012).
- <sup>10</sup> D. Y. Zhao, Q. S. Huo, J. L. Feng, B. F. Chmelka, G. D. Stucky, *J. Am. Chem. Soc.*, **120**, 24 (1998).
- <sup>11</sup> R. I. Kureshy, I. Ahmad, N. H. Khan, S. H. R. Abdi, K. Pathak *et al.*, *J. Catal.*, **238**, 1 (2006).
- <sup>12</sup> K. S. W. Sing, D. H. Everett, R. A. Haul, L. Moscou, R. A. Pierotti *et al.*, *Pure Appl. Chem.*, **57**, 4 (1985).
- <sup>13</sup> K. Bendahou, L. Cherif, S. Siffert, H. L. Tidahy, H. Benassa *et al.*, *Appl. Catal. A: Gen.*, **351**, 1 (2008).
- <sup>14</sup> J. C. Groen, L. A. A. Peffer, J. Pérez-Ramírez, *Micropor. Mesopor. Mat.*, **60**, 1 (2003).
- <sup>15</sup> B. Scholze, D. Meier, *J. Anal. Appl. Pyrol.*, **60**, 1 (2001).
- <sup>16</sup> H. S. Heo, S. G. Kim, K. E. Jeong, J. K. Jeon, S. H. Park *et al.*, *Bioresour. Technol.*, **102**, 4 (2011).
- <sup>17</sup> S. H. Lee, H. S. Heo, K. E. Jeong, J. H. Yim, J. K. Jeon *et al.*, *J. Nanosci. Nanotechnol.*, **11**, 1 (2011).
- <sup>18</sup> J. Adam, M. Blazso, E. Meszaros, M. Stocker, M. H. Nilsen *et al.*, *Fuel*, **84**, 12 (2005).
- <sup>19</sup> H. J. Park, H. S. Heo, J. K. Jeon, J. Kim, R. Ryoo *et al.*, *Appl. Catal. B: Environ.*, **95**, 3 (2010).
- <sup>20</sup> F. Shafizadeh, Y. Z. Lai, *J. Org. Chem.*, **37**, 2 (1972).
- <sup>21</sup> J. B. Paine, Y. B. Pithawalla, J. D. Naworal, *J. Anal. Appl. Pyrol.*, **83**, 1 (2008).
- <sup>22</sup> Q. Lu, W. M. Xiong, W. Z. Li, Q. X. Guo, X. F. Zhu, *Bioresour. Technol.*, **100**, 20 (2009).
- <sup>23</sup> A. Pattiya, J. O. Titiloye, A. V. Bridgwater, *J. Anal. Appl. Pyrol.*, **81**, 1 (2008).
- <sup>24</sup> Q. Lu, Z. Tang, Y. Zhang, X. F. Zhu, *Ind. Eng. Chem. Res.*, **49**, 6 (2010).